




# Repurposing metal additive manufacturing support structures for reduction of residual stress deformation

Lucas M. Morand<sup>1</sup> · Joshua D. Summers<sup>2</sup> · Garrett J. Pataky<sup>1</sup> 

Received: 12 October 2021 / Accepted: 28 December 2021 / Published online: 10 January 2022  
© The Author(s), under exclusive licence to Springer-Verlag London Ltd., part of Springer Nature 2022

## Abstract

Support structures in additive manufacturing (AM) have traditionally been implemented to address process restrictions. This study repurposed the supports as design tools to be used to reduce deformation from residual stress in metal AM prints. Four geometric features were selected via industry interviews and simulations, and experimental prints were used to verify the use of new, novel supports addressing both mechanical and process limit needs. These supports reduced maximum deformation by 14.6% in a validation part simulation that contained all four features. Guidelines were created to present the new design envelopes for each geometric feature to aid in the growth of support structure documentation in AM. Using supports to reduce deformation presents a new design tool to AM engineers that allows them to retain critical part geometry and only change support design.

**Keywords** Additive manufacturing · Residual stress · DMLM · Support structures

## 1 Introduction

Additive manufacturing (AM), the umbrella term covering many different technologies and approaches, uses computer instructions to place material in a layer-by-layer fashion [1–4]. The opportunities created by AM, such as increased design freedom, mass customization, designed material possibilities, and part consolidation, have fueled the growth of this family of processes, thereby branching into different subsets [5]. Selective laser melting (SLM) is an approach within powder bed fusion (PBF) that uses a laser to fully melt the powder at each layer [6]. Within SLM is direct metal laser melting (DMLM) which operates on metal powders. This process can achieve up to 99.9% relative density, allowing AM parts to rival the more isotropic characteristics of cast parts while maintaining design freedom associated with AM [6]. This motivates the use of the process despite its challenge of thermal gradient-induced residual stress and part deformation. In this study, support structures are

leveraged for specific geometric features to deal with both their mechanical needs and print limitations. These structures are shown to reduce maximum and average deformation in print while balancing support material use and support removability.

In DMLM, the full melting of the powder and the part geometry affect the cooling rate of the part [7]. As the laser heats an area of the powder, the surrounding area experiences thermal expansion and compresses. As the part cools and shrinks following solidification, it experiences a tensile state [8]. Variables such as the build chamber temperature or thick/thin transitions in the part geometry keep the resulting part mass in compression with a surrounding shell in tension [9, 10]. This can lead to detrimental part deformation and, in severe cases, cracking. While DMLM faces some costly challenges, the advantages enabled by the process motivate the continued development and use of the technology.

The design freedom afforded by AM present the opportunity to address the concerns of residual stress and part cracking through innovative support structure design. Traditionally, support structures are required to aid the material deposition process as each layer needs something below it. Many times, this is required due to features in the component geometries, such as overhangs, bridges, and holes, as the support structures must fill a void and allow a layer to be deposited [11]. For example, a maximum allowable

✉ Garrett J. Pataky  
gpataky@clemson.edu

<sup>1</sup> Department of Mechanical Engineering, Clemson University, Clemson, SC 29634, USA

<sup>2</sup> Department of Mechanical Engineering, University of Texas at Dallas, Richardson, TX 75080-3021, USA

overhang of  $45^\circ$  was experimentally determined in SLM as the steepest that a surface can be [12, 13]. Supports were shown in a previous study to affect a part's post-print deformation as well as the location of maximum deformation [14]. The observation of this phenomenon served as the foundation to explore which combinations of supports and part geometry features reduced deformation in order to provide guidance for implementation.

## 2 Material and methods

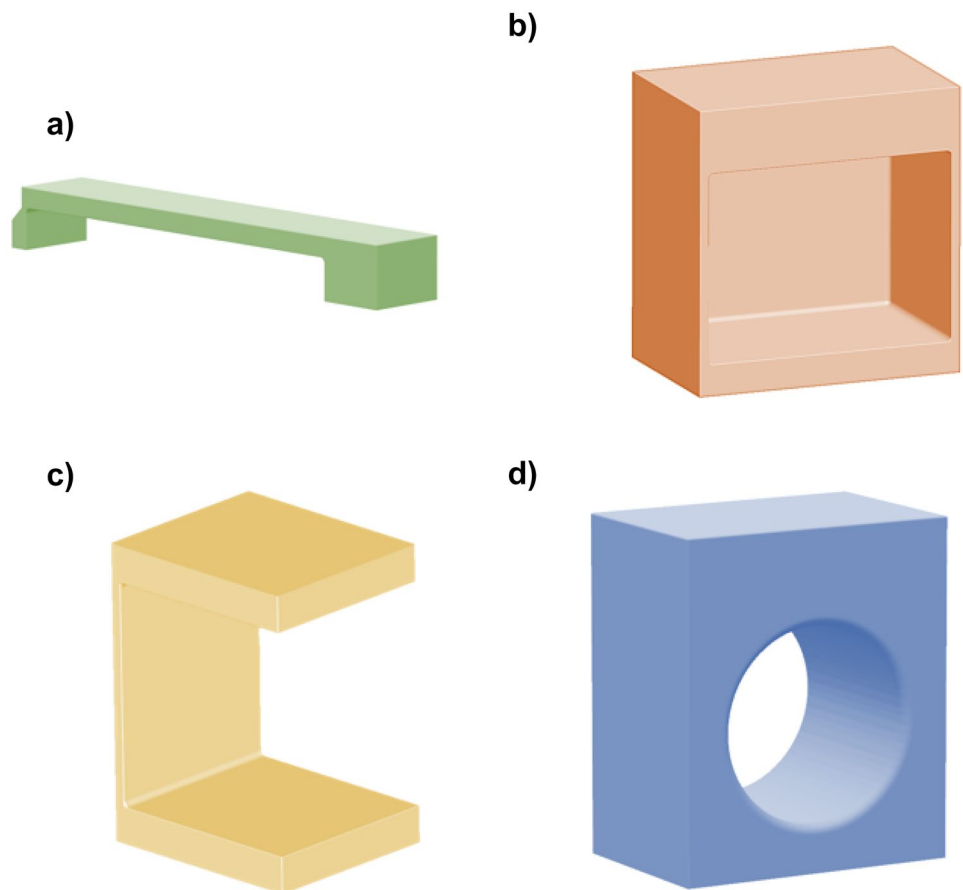
To identify geometries that would benefit from having a customized support structure, interviews were conducted with stakeholders in the AM process at a major energy original equipment manufacturer (OEM). The population consists of eight AM engineers, two design engineers, and two shop technicians. They were interviewed to understand challenges faced both upstream (by designers) and downstream (by technicians) for better context. The interviewees were presented up to six sample parts and asked to identify features of concern if the part were to be printed. Using the results of the interview, the most common features were extracted based on number of times identified

and named based on the language used to describe them. This yielded the four features: bottom surface, roof, overhang, and hole.

Based on the features identified during the interviews, testable, simplified versions were modeled for simulation, analysis, and print. First, the bottom surface was modeled with a size of  $72 \times 12 \times 9$  mm. This was a scaled version of a common geometry used in calibration of print software [15]. The roof was created as  $45 \times 43 \times 27.5$  mm. It used a 25-mm deep recess with 1.5-mm-thick side walls and 2.5-mm-thick rear wall. The overhang was  $40 \times 25 \times 30$  mm with a 1.5-mm-thick vertical wall and 5-mm-thick horizontal members. Finally, the hole was modeled as  $26.25 \times 22.5 \times 15$  mm with a 15-mm-diameter cavity. It had 3.5 mm of material from the edge of the hole to the bottom and 7.5 mm from the edge of the hole to the top of the part. These are shown in Fig. 1.

The baseline supports for each geometry were modeled using the currently accepted approach at the energy OEM. These supports were designed to address only process restrictions while using minimal material, the current best practice approach. Thin plates of varying lengths and toothed vertical ends, for ease of hand removability, were chosen with spacing based on machine limits. These baseline supports are shown for each of the focus geometries in Fig. 2.

**Fig. 1** The modeled focus geometries: **a** bottom surface, **b** roof, **c** overhang, and **d** hole



## 2.1 Experimental setup

To compare the printed parts to their nominal designed dimensions, a common industrial blue light scanning solution was employed. This is a non-contact measurement technology that uses light and reflection to generate point clouds that are used to create a boundary representation model of the part, with map resolutions of 0.025–0.097 mm and measurement accuracies of 0.002–0.008 mm depending on hardware [16]. The 3-dimensional surface was overlaid onto the original CAD model of the geometries to quantify any deviations that occurred from part deformation. Targeted point locations are directly compared across parts and used for average and maximum calculations.

The parts were printed on a commercially available, high-volume DMLM machine. The machine is dual laser powered and features some customizations by the energy OEM. The powder for the parts was a nickel-based super alloy, with a print profile specified by the OEM. Details regarding the specific hardware and material are omitted per the OEM's discretion. DMLM is often used with nickel-based superalloys, such as Haynes 282, Inconel 718, Waspaloy, and MAR M-247, due to their desirable properties in high-temperature applications [17–19]. This family of materials is mechanically and chemically stable at high operating windows often found in aerospace and power-generation applications, offering favorable strength, creep, fatigue, oxidation, and corrosion properties [19, 20]. The presence of large amounts of small, spherical, and coherent  $\gamma'$  precipitates enables the high-temperature creep properties needed in energy applications [21, 22]. Their continued development is crucial to these industries and unlocks performance that is not achieved with other materials and geometries. The as-built parts can be seen still attached to the build plate in Fig. 2.

## 2.2 Computational setup

To understand how the focus geometries would behave, a commercially available print simulation software was used. The expensive nature of DMLM discourages trial-and-error

approaches to understanding print behavior, so simulation software that presents holistic information on the part is especially useful [23]. Many software packages allow for the modifications of inputs to accurately match the hardware and material used in the physical print in order to ensure accuracy in the results. The software used in this study was modified to include the specific machine, laser, and material properties into one pre-determined profile by the OEM. The voxel size of 0.5 mm was held constant for all geometries in order to balance accuracy and computational load. The software simulated the print layer-by-layer and outputted multiple results, including internal stresses induced during the build and resulting displacement. The stress analysis was used to understand the presence of any stress concentrations in the geometries and whether they manifested as compressive or tensile. Secondly, displacement analysis highlighted where each focus geometry deviated from the model after removal from the build plate. These results aided in understanding the behavior of the parts during the print process and after prints.

In an initial study, parts were printed and then scanned using the blue light process [24]. This served to compare the as-built parts to the simulation and evaluate software accuracy. The simulation parameters were the same as the print parameters, and a comparison in results for the roof geometry is shown in Fig. 3. The deformations measured from the printed part showed similar amounts and locations as those predicted by the simulations. Both showed maximum compressive deformation of around 0.2 mm along outer edges and the upper corners of the vertical walls. The software helped to gain both a qualitative and quantitative understanding of part behavior.

## 3 Results

### 3.1 Focus geometry design envelopes

The support structures were designed based on two requirements: (1) a mechanical need or (2) a process limit. The

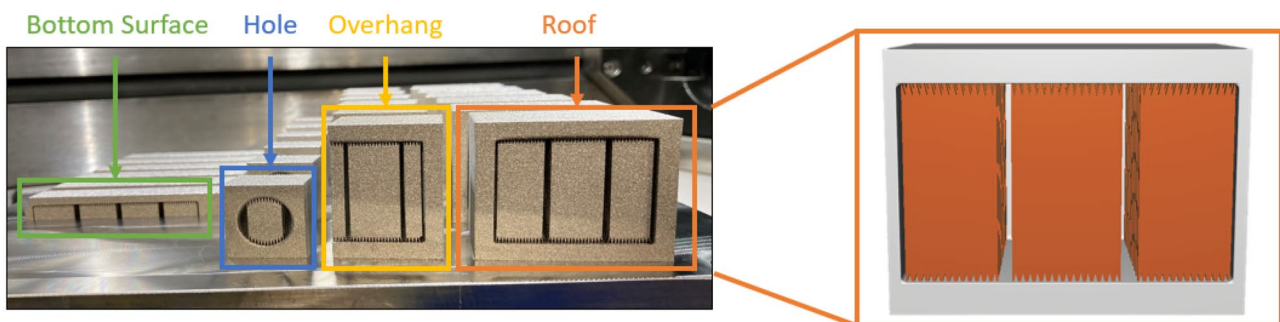
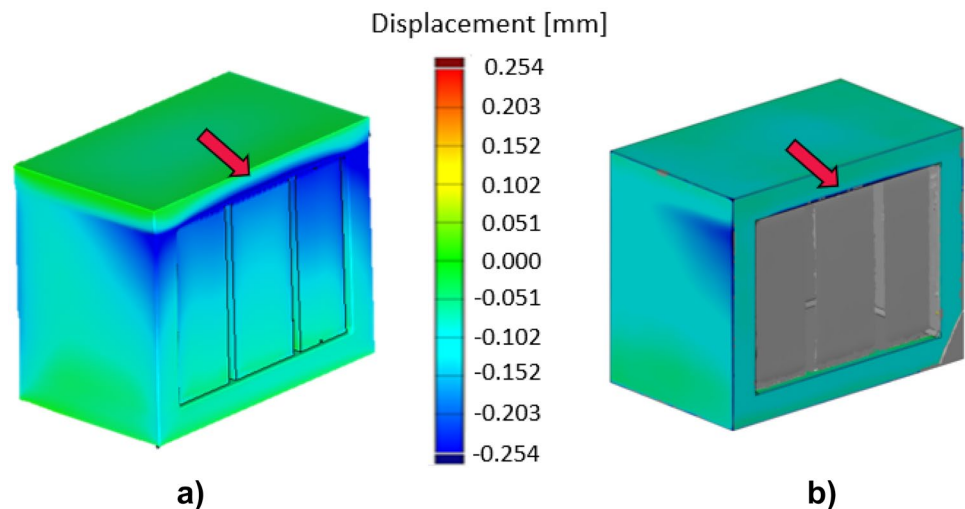


**Fig. 2** Baseline prints still attached to build plate. Thin, toothed supports shown in orange on the modeled roof geometry

**Fig. 3** The **a** simulation and **b** scan of print of the supported roof geometry. The major disagreement is shown with the red arrow



former is based on the previously described challenge of non-uniform cooling faced by DMLM while the latter is a product of placing material additively. When a surface cools faster than its surroundings, it creates tension in the part. A support intended to address this behavior must be designed differently than a support defined by process limits. Each challenge geometry was defined with a design envelope divided into areas based on their needs. Supports were then designed to address the challenges within that envelope. The mechanical need superseded the process need, as it addressed both stress and the process, i.e., it would be load bearing. Two simple example supports were manually designed for each geometry based on mechanical intuition in accordance with the design envelopes.

While these supports are intended to reduce part deformation, two additional metrics were considered: support volume and support removability. If the volume of the support was minimized, then material use and print time were also reduced — both beneficial to the manufacturer. The removability of the supports from the part was also crucial. Producing parts that require extensive manual labor or machining negates the advantages of a digital process and should be avoided. To aid this, toothed connections were used at all support-part interfaces. The success of the support structures was therefore evaluated in deformation amount, support volume, and support removability.

### 3.1.1 Bottom surface

The first geometry, the bottom surface, was characterized as requiring supports that connected the part to the plate (part-to-plate) and as having two sharp corners with two open sides. It was expected to bow convexly with the middle

portion putting supports below in compression while the sides closest to the vertical walls put the supports in tension. This led a design envelope showing mechanically driven supports along the entire length of the part, as is shown in Fig. 4a. Two contrasting strategies were developed for this envelope: block-majority, and plate-majority. The plate portion used plates similar to the baseline, but with a thicker center plate to further reduce any movement and increase adhesion to the build plate. The box portion used a checkerboard pattern of square cross-section columns. Both are shown from a top-down view in Fig. 4a. In simulations, the block-majority did not reduce deformation, so it was not further developed.

### 3.1.2 Roof

The roof needed supports spanning a space within the part (part-to-part) and had four sharp bends making a rectangle, with only one open side. It experienced movement in two directions. First, the upper horizontal member created tension at the portion furthest from all three vertical walls. Then, the two vertical walls bent inward, subjecting the upper horizontal member to compression. As such, mechanical-based supports to address the two movements are shown in Fig. 4b with the resulting process limit needs shown in blue.

The support strategies for the roof included the “Y” and the beam configurations. First, the Y interfaced with the top corners of the roof then came down to the base at an angle defined by process limits. It was solid in the shape of the Y, with plates in the valley of the Y. The solid shape kept the vertical walls from compressing inward, while the plates in the valley kept the top vertical component

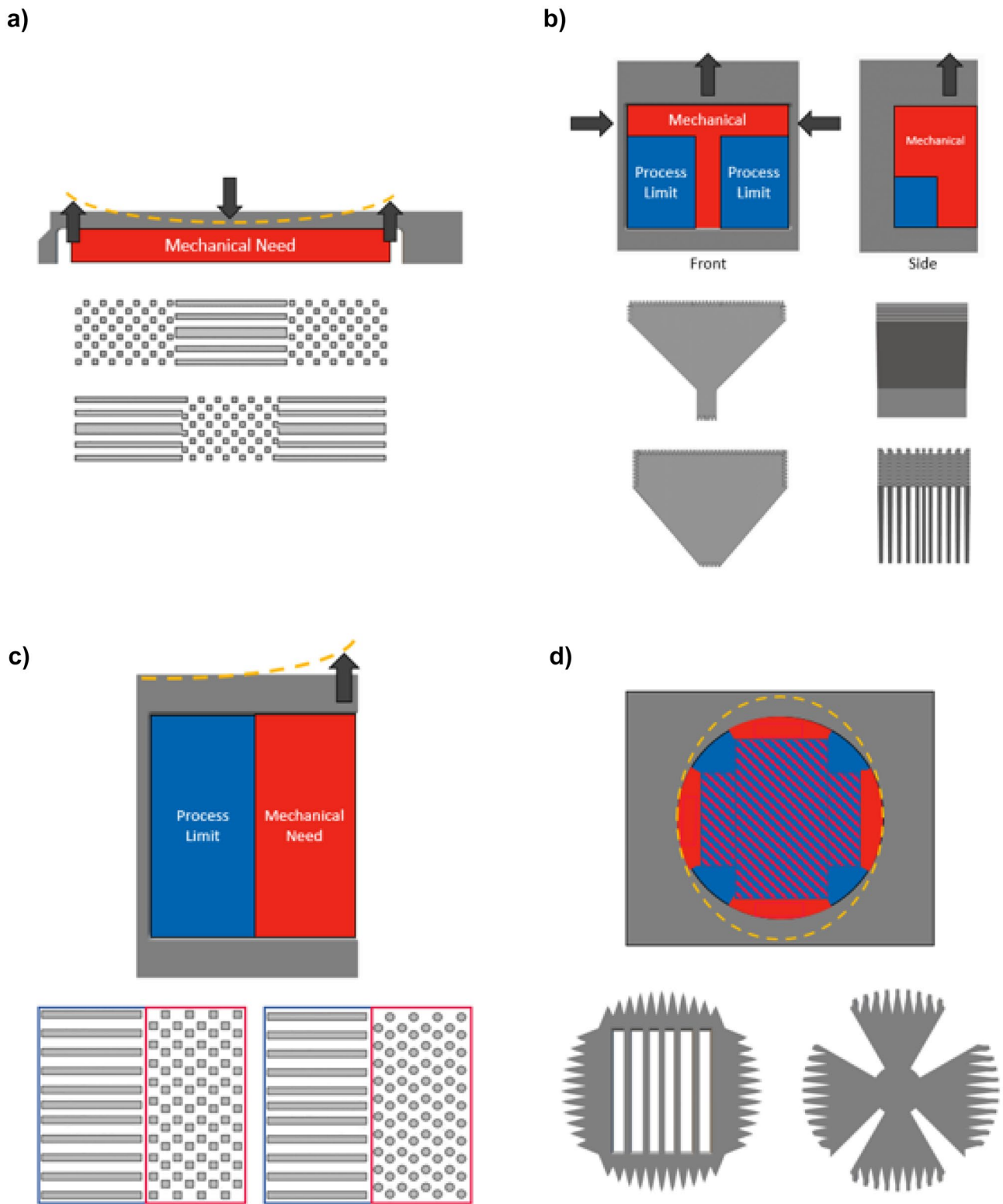


**Fig. 4** Design envelopes and example supports for each geometry. **a** Bottom surface supports in top view, **b** roof supports in front and side views, **c** overhang supports in top view, **d** hole supports in front view

of the roof from peeling upward and addressed process limits. The plating was designed to reduce material use in regions where the mechanics need was not as great. The beam approach addressed the vertical wall movement more directly with a solid bar across the top of the cavity as that was where the deformation was most prevalent. This bar was normal to the walls, unlike the Y that was around a 45-degree incline. This addresses the deflection orthogonally instead of in one of two components. The beam used plates at an incline underneath the bar to minimize material use where movement prevention was not as crucial. These two strategies were further developed into different derivations. First, they were both fully plated to improve material use and removability because the solid sections in both the Y and beam proved to greatly increase support volume and make removal difficult. The geometry of the roof made it incapable of using wire electrical discharge machining (EDM) to remove the supports, emphasizing the importance of ease of removability of the supports. Then, the beam was also modeled with holes in the lower portion to further reduce material use in areas of low mechanical need.

### 3.1.3 Overhang

The overhang geometry required part-to-part supports and featured two sharp corners but with only one vertical side. Removing the top beam of the overhang geometry and isolating it in two dimensions yielded a free-body diagram of a simple cantilever beam. Using this, the horizontal placement of the support reactions along the beam did not affect the reactionary normal force because they had no term addressing the length of the beam. However, the magnitude of the moment at the fixed end decreased as the support reactions were placed further away. Therefore, the region of most mechanical influence was furthest away from the vertical wall. The movement in this zone created tension, as shown in red in Fig. 4c. The remaining region was dictated by the process limits shown in blue. These were addressed with two options: boxed column and cylindrical column. On both, the half of the region closest to the vertical wall was less critical to support and designed on a process limit basis with minimal plates. The other half featured either box or circle cross-section columns. These columns were identical in volume, although the cylinder strategy had more columns than the box because of the minimum space required between columns by process limits.

### 3.1.4 Hole

Finally, the hole necessitated part-to-part supports but with a circular void completely through the body. It was simplified

to a hole in uniaxial tension. Estimating the deformation with Kirsch's solution [25], the regions of most importance to support were the  $0^\circ$  and  $180^\circ$  regions in tension and the  $90^\circ$  and  $270^\circ$  regions in compression as shown in Fig. 4d. Similar to the overhang, this geometry also had a large volume to be managed by process limit supports in the center. This area needed to complement the red regions on the vertical and horizontal lines while being mindful of material use, as shown in the hatched coloring in the figure. This was done through a box support strategy and a cross support strategy. Both placed solid supports preventing the tension and compression at the  $0^\circ/180^\circ$  and  $90^\circ/270^\circ$  regions, respectively. However, the inner region served as the main differentiating factor. The box used rectangular slots spaced by process limits for material reduction while the cross used a shape resembling a cross, as shown in Fig. 4d.

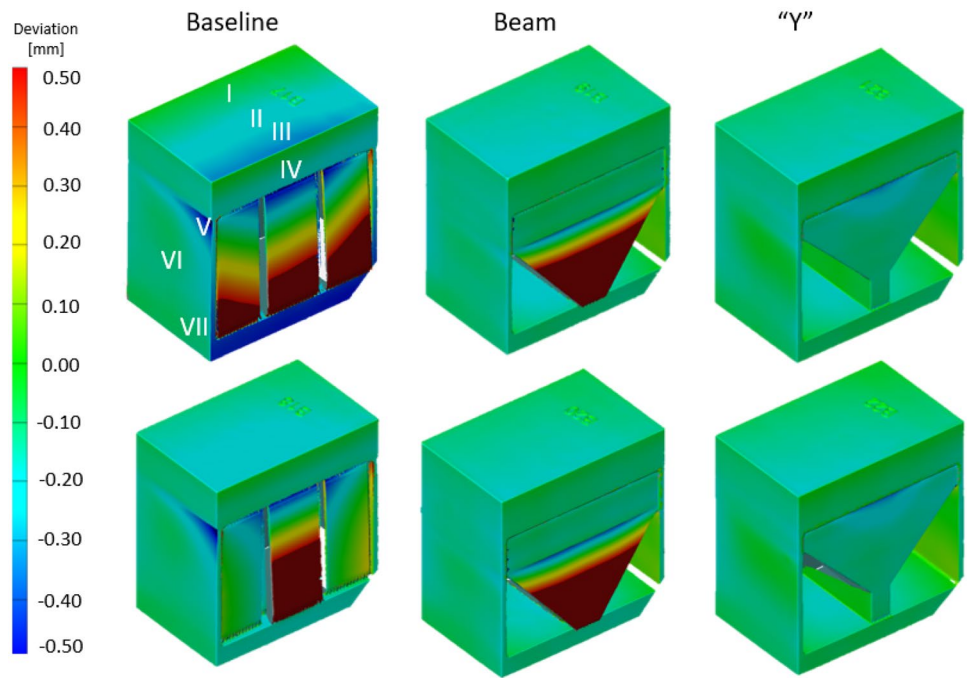
## 3.2 Prints of test geometries

Each part was printed to assess the impact of the support structures on part deformation. For the bottom surface, a common method of measuring the effect of residual stress is to measure the vertical displacement when partially cut along the length of the supports with a wire EDM [23]. The advanced support strategy, plate-majority, decreased the curl height by 0.95% compared to the baseline supports.

The parts were removed from the build plate and scanned with blue light to compare maximum and average deformations on each geometry. Based on the simulation results, seven areas of interest were studied during the blue light measurements. One of the geometries, the roof, shows the seven measurement points and comparison between the baseline, beam, and Y supports in Fig. 5. Improvements at points III and V are apparent between the baseline and both advanced supports. Parts were scanned again once the supports were removed. The average of the seven points was used to give an average deformation value to the geometry. Each geometry was printed twice on the same build plate, with the average of each pair used to compare across supporting strategies. Similarly, each part had a maximum deformation value. The average maximum deformation of a pair of prints was used for comparison.

All advanced strategies reduced the average deformation of the parts after support removal. The maximum deformation was also reduced in all cases except the overhang with box supports. The improvements were shown across all of the geometries, with the beam-plate reducing average deformation by 39.79% and maximum deformation by 59.57% and the Y-plate by 43.60% and 57.45%, respectively. The deformation reduction for the beam-plate was 13.65% for average and 49.49% for maximum while the Y-plate was 32.10% average reduction and 58.59% maximum reduction. All of the metrics of success

**Fig. 5** Deviation from the CAD model of the roof geometry with common measurement points shown in white numerals on the first baseline scan



are summarized in Table 1. The removability score was assessed by a field expert at the OEM.

### 3.3 Combination part validation

The simulation and experimental results verified the reduction in deformation for customized supports. However, each of these cases was isolated features. To validate them in an engineering or industrial context where these

concepts are meant to be used, the strategies were used on a 140×80×40-mm crank plate from a manual crank assembly that included each of the features of interest. This part is shown in Fig. 6.

The demonstration part was first supported with the same baseline supports as previously used in the research that were commonplace for the energy OEM. These were uniformly distributed flat plates with teeth at part interfaces. Their design was centered around that of the traditional

**Table 1** Comparison of deformation results, volume, and removability metrics for each geometry. Measured values are compared to the baseline

Geometry	Support	Simulation	Support Removal		Volume Change	Removability
		MAX	MAX	AVG		
Bottom Surface	Baseline	-	BL	Height	-	●●
	Plated	-18.90%	-6.06%	-0.95%	11.10%	●●●
	Block	55.20%			-13.40%	●●●
Hole	Baseline	-	-	-	-	●●●
	Box	-14.30%	-15.15%	-24.59%	51.50%	●
	Cross	-17.90%	-24.24%	-21.31%	96.40%	●
Overhang	Baseline	-	-	-	-	●●
	Box	-42.40%	11.93%	-5.71%	9.50%	●●●
	Cylinder	-41.90%	-3.67%	-11.21%	10.90%	●●●
Roof	Baseline	-	-	-	-	●●●
	Y	-40.30%			37.30%	●
	Y-Plate	-22.40%			-23.30%	●
	Beam	-37.30%			52.40%	●
	Beam-Plate	-20.90%	-49.49%	-13.65%	3.60%	●●●
	Beam-Hole	-28.40%	-58.59%	-32.10%	23.90%	●

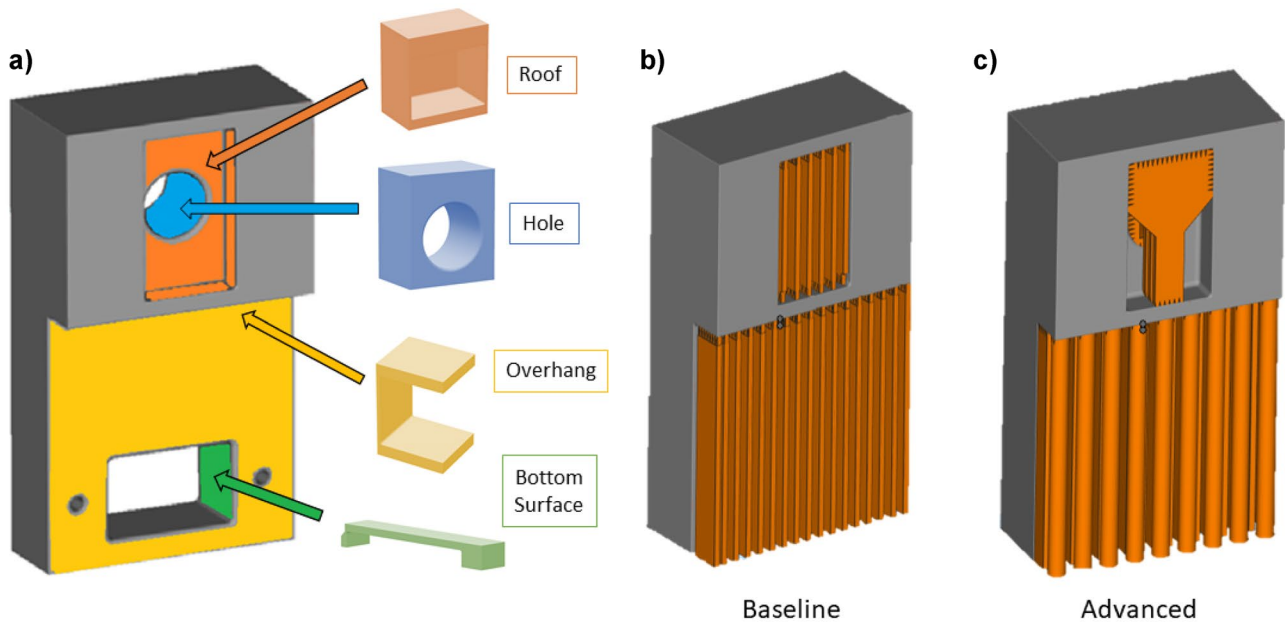


**Fig. 6** a Demonstration part highlighting all the combined challenge features. b The baseline supports applied to the part. c The new, advanced supports applied to the part

support role: minimizing material use as well as print and post-processing time. This contrasts with the advanced supports designed based on the design envelopes.

The advanced part used the most promising support structure from each individual feature. For the bottom surface, a plate-column-plate pattern was used to address sagging resulting in alternating tension–compression–tension. The roof was supported by a plated Y to minimize material use and increase removability while still concentrating on the compression of the vertical walls and the tension of the top wall. The overhang addressed the vertical tension caused by the part’s movement by using columns at the free end and process-limit–defined plates between the columns and the vertical wall. Finally, the hole interfaced with the part at the sides and top/bottom as described in the design envelope with slots in the center for less material use. All interfaces between part and support used teeth to facilitate removal of the supports in the case of a print.

The baseline supports resulted in a total volume of 52,290 mm<sup>3</sup> while the advanced supports used only 14.5% more material at 59,893 mm<sup>3</sup>. In print simulations, the advanced supports had 14.6% less maximum deformation post-print after support removal.

## 4 Discussion

### 4.1 Deformation reduction

The work presented attempts to address the challenge of part deformation in metal AM. Using customized supports to

address part deformation is an unexplored area that allows AM designers to retain the necessary part geometries and change only part supports to print successfully. Reducing part deformation in the design phase minimizes the number of print-and-check iterations needed, further improving the lower design cycle time that is a key driver of AM use. A reduction in part deformation and eliminating part failure on the build plate keeps more AM parts within design tolerance, reducing the number of scrapped parts not meeting requirements. In addition, part deformations that are drastic enough to cause machine collisions and recoater tears further increase AM costs. Cost models show that indirect costs, such as the time associated with the pre- and post-processing, are a key driver in AM costs [26]. More thorough models that include ill-structured costs will account for factors such as waste and show the importance of reducing scrap [27]. One model even factors for up to seven times the material use to fully account for scrap waste [28]. Defects that can be prevented through re-work do prevent scrap waste, but the operations then increase in-direct costs. Being able to better control the part deformation serves to ensure more prints are successful and cost-effective. While AM’s advantages have been discussed in one-off parts and small-batch productions, reducing the unit cost will increase its competitiveness against established manufacturing methods that enjoy the economies of scale [29]. The reductions of deflections shown in this paper, with the bottom surface reducing by 6.06% (maximum vertical deflection), the overhang by 11.21%, the hole by 24.59%, and the roof by 32.10%, show a move in this direction.



The parts were scanned and measured via blue light immediately after removal from the build plate and then again after the supports were removed. The roof parts with beam, Y, beam-hole, and one beam-plate support were not able to have their supports removed. This reflected the importance of the success metric of removability as even if those parts had shown zero deformation, they would still be unusable because the supports could not be removed. For the remaining parts, some support removals caused changes in part deformation. The hole geometries both showed less deformation after support removal than after removal from the build plate. Conversely, the overhang with box supports saw worse maximum deformation after support removal than when measured after removal from the build plate. The deformation of the beam supports in Fig. 5 compared to the Y supports is an example of different supports’ reactions to residual stress. This highlights that deformation still affects the part even after the build process is complete, and it opens the door for further research on stress-reducing post-processing methods. Some simulation software also offer results for these intermediate steps with the part pre- and post-support removal, as well as different post-processing steps [23]. Stress analysis in AM does not conclude once the build of the part is complete as this is often not the end-use geometry.

#### 4.2 Guideline creation and advanced support geometry

Guidelines are commonly found in many areas of design [30–33]. The creation of guidelines supports the standardization

of work and creates more consistent and less subjective work. With AM being a young process relative to other manufacturing methods, inexperienced engineers joining the field do not have the same number of resources as available in more established manufacturing processes. Guidelines were developed to help fill the need for resources for young engineers as well as formally present new information to experienced engineers. Based on the findings detailed above, the guidelines were created based on a modified version of the Unit Cell Design Guideline Development Method [34]. Modifications were made to a geometry, then simulations and prints demonstrated changes in behavior, so an if–then relation was created. If one of the features is seen in a part, then the design envelope and suggested supports are presented. The guideline for the bottom surface feature is shown in Fig. 7.

The creation of guidelines supports the standardization of work and creates more consistent and less subjective work. Subjectivity has been shown in guideline implementation, with inexperienced designers creating different structures than their more experienced counterparts [34]. As more solution supports are generated and the understanding of the print behavior improves, the design envelopes will be narrowed, and the support designs will converge. Furthermore, this guideline development structure is not confined strictly to DMLM or nickel-based materials but instead lends itself for continued growth to parallel that of AM.

In this study, simple example support structures were manually created from solid mechanics intuition and previous results to satisfy the needs of each geometry according

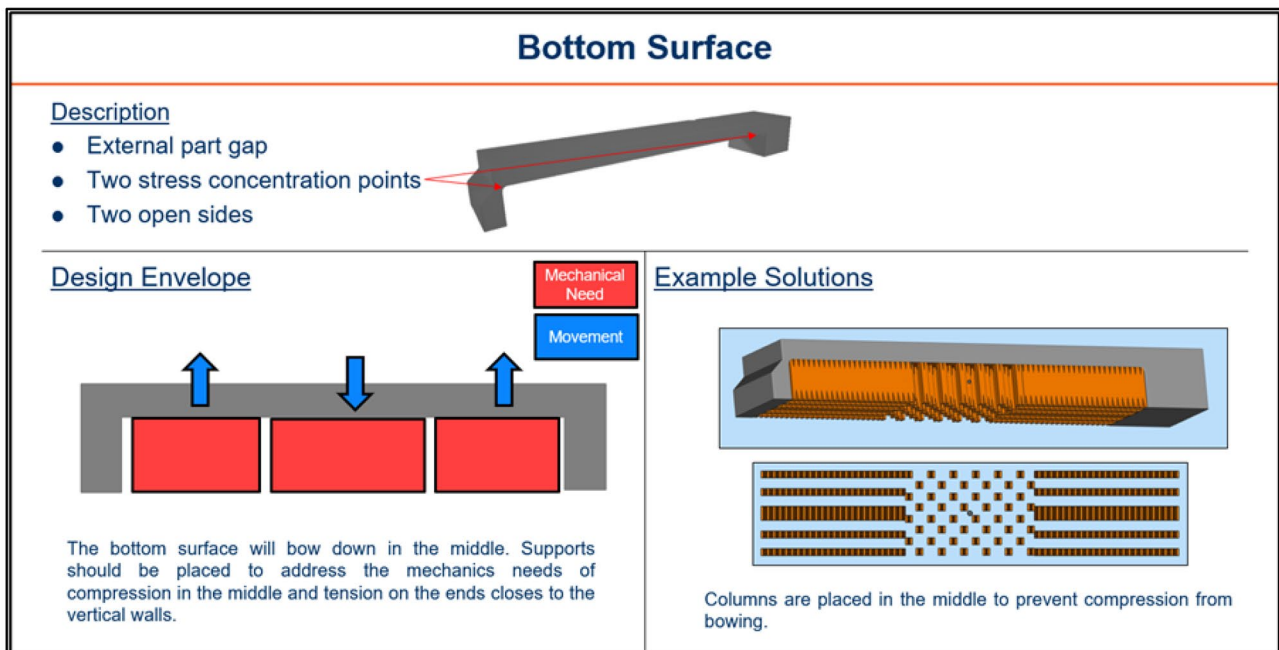


Fig. 7 Guidelines generated for the bottom surface geometry

to the design envelopes. In common commercial AM preparation software, support generation often involves simple plates, block, columns, and gussets [11]. Research is being conducted in generating cellular structures that better utilize the design freedoms and complexity capabilities of AM [11]. Optimization tools are also being applied to the supports in order to minimize the traditional targets of print time and material use [35]. Combining these two research threads leads to the use of topology optimization to design advanced support geometries such as gyroids that are functionally graded [36–39]. Integrating these technologies with the described design envelopes shown in the guidelines would reduce both deformation and material use by addressing the specific needs of different features of a part with the optimized and advanced support geometries. Rather than using optimization metrics such as heat conduction or surface finish, the equations can be tailored to each part based on the understanding of the deformation presented in the guidelines [36, 39].

## 5 Conclusions

This work redefines support structures as design tools rather than the necessary waste they were considered as previously. Traditionally, supports were placed in a constant and consistent fashion as defined by process limits, with revisions being made to the part geometry to ensure a successful print. Instead, it is shown that support structure design is an active and intentional process that positively impacts part deformation. The placement and shaping of supports are key parameters to a successful print. This is demonstrated in defining supported regions as either mechanically driven or process limit driven and encouraging the application of a varied support layout within the same part region, a novel approach to supporting parts in metal AM. Different features have distinct needs and should be supported as such. This work presents supports as a new tool to AM engineers that enables them to reduce part deformation without affecting the shape of the part that is already defined by design requirements.

**Acknowledgements** Simulations and print preparations were completed on hardware provided by the OEM. Printing and post-processing occurred at the OEM.

**Author contribution** Lucas Morand: modeling, simulation, analyses, original draft. Joshua Summers: reviewing, editing, supervising. Garrett Pataky: reviewing, editing, supervising.

**Funding** This work was supported by General Electric Company through sponsor project #2014149. Any opinions, findings, and conclusions are those of the authors and do not necessarily reflect the views of the sponsor.

**Availability of data and materials** Not applicable.

**Availability of code** Not applicable.

## Declarations

**Ethics approval** Not applicable.

**Consent to participate** Not applicable.

**Consent for publication** Not applicable.

**Competing interests** The authors declare no competing interests.

## References

1. Monzón MD, Ortega Z, Martínez A, Ortega F (2015) Standardization in additive manufacturing: activities carried out by international organizations and projects. *Int J Adv Manuf Technol* 76:1111–1121
2. Savini A, Savini GG (2015) A short history of 3D printing, a technological revolution just started. In: 2015 ICOHTEC/IEEE International History of High-Technologies and their Socio-Cultural Contexts Conference (HISTELCON), pp 1–8
3. Horvath J (2014) A brief history of 3D printing. In: Horvath J (ed) *Mastering 3D Printing*. Apress, Berkeley, CA, pp 3–10
4. Shahrudin N, Lee TC, Ramlan R (2019) An overview on 3D printing technology: technological, materials, and applications. *Procedia Manuf* 35:1286–1296
5. Thompson MK, Moroni G, Vaneker T et al (2016) Design for additive manufacturing: trends, opportunities, considerations, and constraints. *CIRP Ann* 65:737–760. <https://doi.org/10.1016/j.cirp.2016.05.004>
6. Yap CY, Chua CK, Dong ZL et al (2015) Review of selective laser melting: materials and applications. *Appl Phys Rev* 2:41101
7. Gouge M, Michaleris P (2017) Thermo-mechanical modeling of additive manufacturing. Butterworth-Heinemann
8. Ding J, Colegrove P, Mehnen J et al (2011) Thermo-mechanical analysis of wire and arc additive layer manufacturing process on large multi-layer parts. *Comput Mater Sci* 50:3315–3322
9. Li C, Liu ZY, Fang XY, Guo YB (2018) Residual stress in metal additive manufacturing. *Procedia CIRP* 71:348–353. <https://doi.org/10.1016/j.procir.2018.05.039>
10. Mirkoohi E, Sievers DE, Garmestani H, Liang SY (2020) Thermo-mechanical modeling of thermal stress in metal additive manufacturing considering elastoplastic hardening. *CIRP J Manuf Sci Technol* 28:52–67. <https://doi.org/10.1016/j.cirpj.2020.01.002>
11. Strano G, Hao L, Everson RM, Evans KE (2013) A new approach to the design and optimisation of support structures in additive manufacturing. *Int J Adv Manuf Technol* 66:1247–1254. <https://doi.org/10.1007/s00170-012-4403-x>
12. Atzeni E, Salmi A (2015) Study on unsupported overhangs of AlSi10Mg parts processed by Direct Metal Laser Sintering (DMLS). *J Manuf Process* 20:500–506. <https://doi.org/10.1016/j.jmapro.2015.04.004>
13. Thomas D (2009) The development of design rules for selective laser melting. University of Wales
14. Morand L, Summers JD, Pataky GJ (2021) Exploration of support structure design for additive manufacturing at a major OEM: a case study. In: *Proceedings - ASME 2021 International Design Engineering Technical Conferences and Computers and*

- Information in Engineering Conference. DETC2021-69818. American Society of Mechanical Engineers Digital Collection
15. Jonsson S, Krappedal S (2018) Evaluation of residual stresses and distortions in additively manufactured components. KTH Royal Institute of Technology
  16. Xiao G, Liu S, Zhang Y et al (2021) A measurement method of the belt grinding allowance of hollow blades based on blue light scanning. *Int J Adv Manuf Technol* 116:3295–3303
  17. Deshpande A, Nath SD, Atre S, Hsu K (2020) Effect of post processing heat treatment routes on microstructure and mechanical property evolution of Haynes 282 Ni-based superalloy fabricated with selective laser melting (SLM). *Metals (Basel)* 10:629
  18. Ströbner J, Terock M, Glatzel U (2015) Mechanical and microstructural investigation of nickel-based superalloy IN718 manufactured by selective laser melting (SLM). *Adv Eng Mater* 17:1099–1105
  19. Hagedorn Y, Risse J, Meiners W et al (2013) Processing of nickel based superalloy MAR M-247 by means of High Temperature-Selective Laser Melting (HT-SLM). In: *Proc 6th Int Conf Adv Res Virtual Rapid Prototyp*. pp 291–295
  20. Qiu C, Chen H, Liu Q et al (2019) On the solidification behaviour and cracking origin of a nickel-based superalloy during selective laser melting. *Mater Charact* 148:330–344. <https://doi.org/10.1016/j.matchar.2018.12.032>
  21. Basak A (2019) Additive manufacturing of high-gamma prime nickel-based superalloys through selective laser melting (SLM). *Solid Free Fabr 2019 Proc 30th Annu Int Solid Free Fabr Symp - An Addit Manuf Conf SFF 2019* 554–575
  22. Gribbin S, Ghorbanpour S, Ferreri NC et al (2019) Role of grain structure, grain boundaries, crystallographic texture, precipitates, and porosity on fatigue behavior of Inconel 718 at room and elevated temperatures. *Mater Charact* 149:184–197. <https://doi.org/10.1016/j.matchar.2019.01.028>
  23. Peter N, Pitts Z, Thompson S, Saharan A (2020) Benchmarking build simulation software for laser powder bed fusion of metals. *Addit Manuf* 36:101531. <https://doi.org/10.1016/j.addma.2020.101531>
  24. Morand LM (2021) Development of guidelines for support structure design and placement in metal additive manufacturing. Clemson University
  25. Kirsch C (1898) The theory of elasticity and the needs of strength theory. *J Assoc Ger Eng* 42:797–807
  26. Ding J, Baumers M, Clark EA, Wildman RD (2021) The economics of additive manufacturing: Towards a general cost model including process failure. *Int J Prod Econ* 237:108087
  27. Baumers M (2020) Cost implications of precision additive manufacturing. In: *Precision Metal Additive Manufacturing*. CRC Press, pp 157–170
  28. Gibson I, Rosen DW, Stucker B, Khorsani M (2021) *Additive manufacturing technologies*. Springer
  29. Baumers M, Holweg M (2019) On the economics of additive manufacturing: Experimental findings. *J Oper Manag* 65:794–809
  30. Boothroyd G (1994) Product design for manufacture and assembly. *Comput Des* 26:505–520. [https://doi.org/10.1016/0010-4485\(94\)90082-5](https://doi.org/10.1016/0010-4485(94)90082-5)
  31. Greer JL, Wood JJ, Jensen DD, Wood KL (2002) Guidelines for product evolution using effort flow analysis: results of an empirical study. In: *ASME 2002 International Design Engineering Technical Conferences and Computers and Information in Engineering Conference*. American Society of Mechanical Engineers Digital Collection, pp 139–150
  32. Perez KB, Anderson DS, Wood KL (2015) Crowdsourced design principles for leveraging the capabilities of additive manufacturing. In: *International Conference of Engineering Design*, pp 1–10
  33. Otto K (2001) *Product design: techniques in reverse engineering and new product development*. Prentice Hall, New Jersey
  34. Fazelpour M, Shankar P, Summers JD (2019) A unit cell design guideline development method for meso-scaled periodic cellular material structures. *J Eng Mater Technol* 141:041004
  35. Vaissier B, Pernot J-P, Chougrani L, Véron P (2019) Genetic-algorithm based framework for lattice support structure optimization in additive manufacturing. *Comput Des* 110:11–23. <https://doi.org/10.1016/j.cad.2018.12.007>
  36. Kuo Y-H, Cheng C-C, Lin Y-S, San C-H (2018) Support structure design in additive manufacturing based on topology optimization. *Struct Multidiscip Optim* 57:183–195
  37. Hussein A, Hao L, Yan C et al (2013) Advanced lattice support structures for metal additive manufacturing. *J Mater Process Technol* 213:1019–1026. <https://doi.org/10.1016/j.jmatprotec.2013.01.020>
  38. Cheng L, Liang X, Bai J et al (2019) On utilizing topology optimization to design support structure to prevent residual stress induced build failure in laser powder bed metal additive manufacturing. *Addit Manuf* 27:290–304. <https://doi.org/10.1016/j.addma.2019.03.001>
  39. Malekipour E, Tovar A, El-Mounayri H (2018) Heat conduction and geometry topology optimization of support structure in laser-based additive manufacturing. In: Wang J, Antoun B, Brown E et al (eds) *Conference Proceedings of the Society for Experimental Mechanics Series*. Springer International Publishing, pp 17–27

**Publisher's Note** Springer Nature remains neutral with regard to jurisdictional claims in published maps and institutional affiliations.